

Vesicle–Micelle Transformation of Phosphatidylcholine/Octyl- β -D-glucopyranoside Mixtures As Detected with Titration Calorimetry[†]

Markus R. Wenk and Joachim Seelig*

Department of Biophysical Chemistry, Biocenter of the University of Basel, Klingelbergstr. 70, CH-4056 Basel, Switzerland

Received: March 3, 1997; In Final Form: April 16, 1997[⊗]

The vesicle–micelle transition of lipid bilayers induced by the addition of the nonionic detergent octyl- β -D-glucopyranoside (OG) was studied with high-sensitivity titration calorimetry and spectroscopic methods. Sonified phospholipid vesicles composed of 1-palmitoyl-2-oleoyl-*sn*-glycero-3-phosphocholine (POPC) were titrated into OG solutions with concentrations between 15 and 22 mM. The critical OG concentration for bilayer micellization was determined as $c_b^* = 15.4 \pm 0.3$ mM whereas the critical micellar concentration of pure OG was $c_{cmc} = 23.7$ mM (in buffer). All calorimetric titrations were performed below the cmc of pure OG solutions. The titration curves can be explained by a superposition of three processes, namely (i) a partitioning of surfactant molecules into the lipid membrane, (ii) a membrane micellization, and (iii) a membrane re-formation. The basic process is a partitioning of OG molecules into the phospholipid vesicles which occurs during the whole titration experiment. It can be described according to $X_b = Kc_{D,f}$ where X_b is the degree of binding (effective surfactant-to-lipid ratio) and $c_{D,f}$ is the equilibrium detergent concentration free in solution. The thermodynamic parameters were determined as $K = 88 \pm 3$ M⁻¹ and $\Delta H_D^0 = 1.7 \pm 0.4$ kcal/mol for the transfer of OG from the aqueous phase to the membrane ($15 \text{ mM} \leq c_D^0 \leq 22 \text{ mM}$). OG partitioning entails a bilayer micellization in the initial phase of the lipid-into-detergent titration experiment. Bilayer micellization is an endothermic process with $\Delta H_{mic} = +1.85 \pm 0.1$ kcal/mol lipid. With continuous addition of lipid, bilayer micellization comes to a halt and is replaced by the reverse process. The demicellization process is exothermic with $\Delta H_{demic} = -1.84 \pm 0.1$ kcal/mol lipid. Micellization and demicellization are thus symmetrical processes. Once the free OG concentration falls below the critical limit of $c_b^* = 15.4$ mM, the titration curves follow the predictions of the partition model. A quantitative model is proposed to describe the excess heat, $\Delta \bar{H}_D^E$, of the bilayer \rightleftharpoons micelle equilibrium. To a first approximation, $\Delta \bar{H}_D^E$ follows the symmetrical mixing behavior of two closely related nonpolar liquids. Phosphorus-31 nuclear magnetic resonance and right-angle light scattering were used to monitor the structural changes of the OG/POPC mixtures. They confirm a phase boundary between the bilayer phase and the bilayer/micelle coexistence phase at $c_b^* = 15.4 \pm 0.3$ mM and $X_b = 1.36 \pm 0.04$. The phase boundary between the bilayer/micelle coexistence phase and the pure micellar phase is found for $X_b \geq 2.8$. The calorimetric titrations can be used to construct a rather precise phase diagram of the POPC/OG system as the discontinuities of the titration curves define the critical concentrations of detergent and lipid at the phase boundaries.

Introduction

Biological membranes are complex assemblies of lipids and proteins. Detergent–membrane interactions are studied in detail since they serve as models for a number of important biological phenomena such as fusion events, anaesthetic action of drugs, or digestion of fat in the intestine.¹ Technical applications such as reconstitution of membrane proteins,² preparation of liposome solutions,^{3,4} or formulations for drug delivery⁵ have further stimulated investigations of lipid–detergent interactions.

A simple scheme for the detergent-induced bilayer solubilization is the so-called “three-stage-model”.^{6,7} According to this model the transfer of detergent from the aqueous phase to the bilayer (stage I) is described by a partition equilibrium. However, only a limited amount of detergent can be accommodated between the lipids. Reaching a critical detergent-to-lipid ratio, the bilayer structure starts to disintegrate. This marks the onset of stage II where detergent–lipid micelles coexist with mixed bilayers. Intermediate structures such as open vesicles,

lamellar sheets, or cylindrical micelles have also been postulated to occur within this phase.^{8,9} Upon further increasing the detergent concentration, the bilayers will finally be completely disrupted (stage III).

The nonionic detergent octyl- β -D-glucopyranoside (OG) has been used extensively for the reconstitution of membrane proteins in functional form due to its nondenaturing effects on proteins and its high critical micellar concentration.¹⁰ In parallel, the physical-chemical properties of OG–lipid mixtures have been studied in detail.^{7,8,11–15} We have recently investigated the partitioning of OG into lipid bilayers composed of 1-palmitoyl-2-oleoyl-*sn*-glycero-3-phosphocholine (POPC) at subsolubilizing OG concentrations.¹⁶ The transfer of OG from the aqueous phase to the membrane could be explained by a surface partition equilibrium. The partition enthalpy, as well as the molar heat capacity were determined by titration calorimetry and were found to be indicative of a hydrophobic binding equilibrium.

In the present study we use high-sensitivity titration calorimetry to quantitatively analyze the vesicle \rightleftharpoons micelle transition of aqueous mixtures of octyl- β -D-glucopyranoside and 1-palmitoyl-2-oleoyl-*sn*-glycero-3-phosphocholine. POPC vesicles,

* Corresponding author. Phone: +41-61-267-2190. Fax: +41-61-267-2189. E-mail: Seelig1@ubaclu.unibas.ch.

[†] Supported by the Swiss National Science Foundation Grant 31.42058.94.

[⊗] Abstract published in *Advance ACS Abstracts*, June 1, 1997.

prepared by sonification, are titrated into OG solutions with high detergent concentrations (i.e. total detergent concentrations $c_D^0 \geq 15$ mM). Under these conditions, the vesicles are disrupted and mixed micelles are formed during the first few injections. However, as more and more lipid is added, the amount of free detergent falls below the critical limit and bilayer micellization is no longer possible. Instead, the reverse process takes place and micelles are dissolved forming again mixed detergent–lipid bilayers. This process continues until all micelles are transformed into bilayers. At the end of the second phase of the titration experiment the solution consists of mixed OG/POPC bilayers in equilibrium with OG monomers. Further addition of phospholipid entails a partitioning of OG monomers into the newly added vesicles combined with a redistribution of OG in existing mixed bilayer aggregates. For the specific conditions investigated, the titration patterns allow a direct visualization of the three stages of the Lichtenberg model, transgressing the phase boundaries in the order III \rightarrow II \rightarrow I. A quantitative analysis is possible in terms of a thermodynamic model which combines the partitioning of detergent into the lipid bilayer with either bilayer micellization or bilayer formation. The titration curves can be explained by the superposition of different enthalpies which are endothermic for OG partitioning into the lipid bilayer and micelle formation but exothermic for the micelle \rightarrow bilayer transformation. The molecular interpretation of the data is confirmed by a simple scheme for the construction of a partial phase diagram from the titration curves.

Materials and Methods

Materials. Octyl- β -D-glucopyranoside (OG) was purchased from Fluka (purity > 99% TLC). 1-Palmitoyl-2-oleoyl-*sn*-glycero-3-phosphocholine (POPC) was obtained from Avanti Polar Lipids (Birmingham, AL). All chemicals were employed without further purification. Buffers were prepared from 18 M Ω water obtained from a NANOpure A filtration system.

Preparation of Lipid Vesicles. Small unilamellar vesicles (SUV) were prepared as follows. A defined amount of lipid (~50 mg) was first dried under a stream of nitrogen, followed by high vacuum for 1 h at room temperature and in the dark. The lipid was then dissolved in dichloromethane (0.5 mL) and again dried under nitrogen. High vacuum was applied overnight. A defined amount of buffer (2 mL) was added to the lipid film, and the suspension was vortexed extensively. Next, the lipid dispersions were sonicated for 20–50 min ($T = 10$ °C) until the solution became transparent. The opalescent solution was centrifuged in an Eppendorf table top centrifuge (8 min at 14 000 rpm) to remove metal debris. Lipid concentrations were determined gravimetrically by carefully weighing the samples and by adding defined amounts of buffer. In separate experiments we have analyzed the lipid content of sonified vesicles with phosphorus analysis. The phosphate analysis yielded a 4.7% (average of 9 determinations) smaller lipid content than the nominal concentration, with maximum deviations between -2 and $+10\%$. The data reported for sonified POPC vesicles were calculated on the basis of the weighing-in concentration.

High-Sensitivity Titration Calorimetry. Isothermal titration calorimetry was performed using an Omega high-sensitivity titration calorimeter from Microcal (Microcal, Northampton, MA).¹⁷ Solutions were degassed under vacuum prior to use to eliminate air bubbles. The calorimeter was calibrated electrically. The data were acquired by computer software developed by MicroCal. In control experiments the corresponding detergent solution (or vesicle suspension) was injected into buffer without lipid (or without detergent). Heats of dilution were

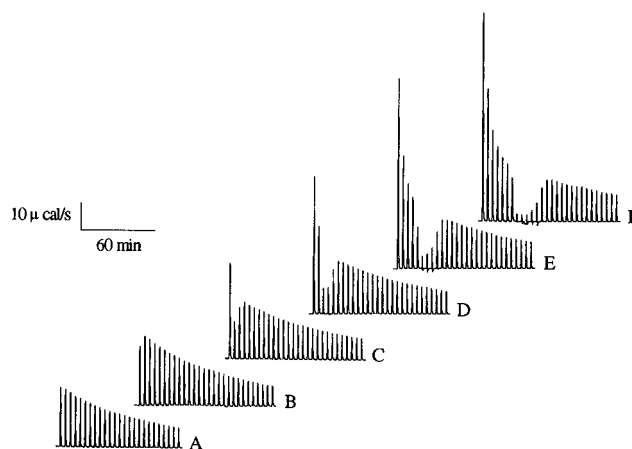


Figure 1. Titration calorimetry of octyl- β -D-glucopyranoside solutions with sonicated vesicles of POPC ($c_L \sim 35$ mM; buffer: 10 mM Tris, pH 7.25, 100 mM NaCl; $T = 28$ °C; vesicle diameter ~ 30 nm). Each peak corresponds to the injection of 10 μ L of lipid suspension into the reaction cell ($V_{\text{cell}} = 1.3353$ mL). The concentration of OG in the reaction cell was (A) 15 mM OG, (B) 16 mM OG, (C) 17 mM OG, (D) 18 mM OG, (E) 20 mM OG, (F) 22 mM OG. Upward peaks denote endothermic reactions.

small compared to the actual measurement but were nevertheless included in the final analysis.

Right-Angle Light Scattering. Light-scattering measurements were made with a Jasco FP 777 spectrofluorometer (Japan Spectroscopic Co., Ltd, Tokyo, Japan) with both excitation and emission wavelengths set at 350 nm, 3 nm slit widths. The sample ($v = 1.5$ mL detergent solution) was continuously stirred and thermostated ($T = 28$ °C). Vesicles ($c_L \approx 30$ mM lipid concentration) were added (10 μ L) using a Hamilton microliter syringe. The scattering intensity at 90° was recorded as a function of time. As a reference, the same experiment was repeated using 1.5 mL buffer without detergent.

NMR Measurements. Solid state ^{31}P -NMR measurements of membranes were recorded at 301 K on a Bruker MSL 400 NMR spectrometer operating at a phosphorus-31 frequency of 161 MHz. A spin echo sequence with gated proton decoupling was used. The recycling delay was 5 s, the $\pi/2$ pulse width 3.05 μ s, and the interpulse spacing 40 μ s. 4000–8000 free induction decays were accumulated. Usually ~ 10 mg of lipid was incubated with a known amount of detergent and mixed in organic solvent. The solvent was evaporated by nitrogen and a small amount (~ 50 μ L) of deuterium depleted water was added. The samples were sealed, subjected to several freeze–thaw cycles and vortexed extensively.

Results

Titration Calorimetry. Figure 1 shows calorimeter tracings of POPC vesicles titrated into OG solutions with concentrations in the range 15–22 mM. The critical micellar concentration (cmc) of OG in water is $c_{\text{cmc}} = 22.6$ mM (at 30 °C).^{18,19} Using the same approach as Paula et al.,¹⁸ we have determined the cmc in buffer (0.1 M NaCl, 10 mM Tris, pH 7.4) as 23.7 mM at 28 °C. The phospholipid titration experiments were thus performed below the cmc of pure OG solutions.

The simplest situation is encountered in Figure 1A where the OG concentration is 15 mM. The detergent is contained in the calorimeter cell ($V_{\text{cell}} = 1.3353$ mL), and 10 μ L aliquots of a phospholipid suspension ($c_L^0 = 29.7$ mM; sonified vesicles, diameter ~ 30 nm) are injected via a Hamilton syringe coupled to a stepping motor. Each injection produces an endothermic heat of reaction, h_i , which decreases smoothly with consecutive injections.

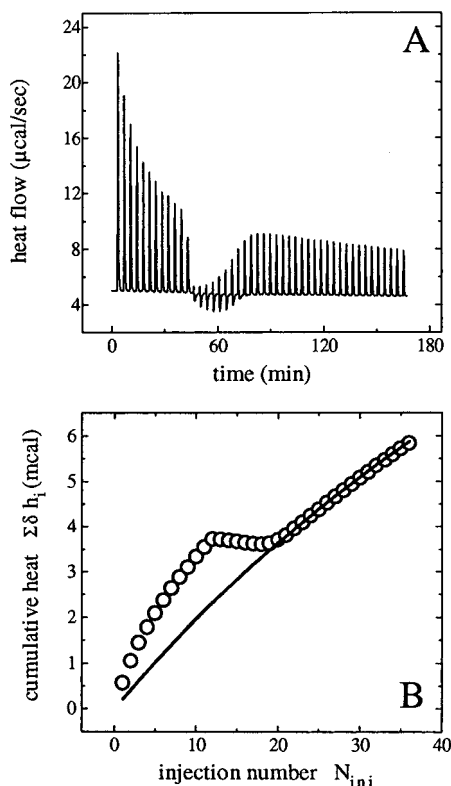


Figure 2. Titration calorimetry of an OG solution with lipid vesicles at solubilizing conditions. (A) Octyl- β -D-glucopyranoside ($c_{\beta}^0 = 19$ mM; buffer: 10 mM Tris, pH 7.4, 100 mM NaCl; $T = 28$ °C; $V_{\text{cell}} = 1.335$ mL) was titrated with POPC SUV ($c_L = 14.35$ mM lipid concentration in the same buffer; $5 \mu\text{L injection}^{-1}$). The reference cell contained buffer. (B) Cumulative heat of reaction (circles) is shown as a function of the injection number. The contribution of OG partitioning (solid line) to the total heat signal was calculated as described in the text using the following parameters: $K = 90 \text{ M}^{-1}$, $\Delta H_{\beta}^0 = 1.75 \text{ kcal mol}^{-1}$. Note the different scales in A and B.

As a control, buffer without lipid was injected into the OG solutions (data not shown). For Figure 1A the heat of dilution, $h_{d,i}$, varied between -6 and $-3 \mu\text{cal}$ per injection. The heat of dilution was subtracted, and the quantitative evaluation of the experimental data was based on

$$\delta h_i = h_i - h_{d,i} \quad (1)$$

Smooth titration curves analogous to that shown in Figure 1A have been observed previously for OG concentrations $c_{\beta}^0 \leq 10$ mM.¹⁶ As will be discussed in more detail below, the titration curve can be explained by a partitioning of OG into the lipid membrane. With each lipid injection the concentration of free detergent is reduced, less detergent is available for binding, and the experimental heat of reaction decreases.

Detergent concentration above 16 mM produce more complicated titration patterns (Figure 1B–F). For $c_{\beta}^0 = 16$ mM only the first titration peak deviates from the otherwise smooth titration curve (Figure 1B). However, at even higher OG concentrations, the titration pattern can formally be divided into three distinct regions as illustrated in detail in Figure 2. For the first N injections, the endothermic heat of reaction decreases monotonously (N varies with the OG concentration). At step $N + 1$ the reaction enthalpy shows a discontinuity. This second phase of the titration experiment comprises again about N injection steps. The reaction enthalpy first drops close to zero and a fast endothermic and a slower exothermic reaction can be discerned. The endothermic enthalpy then increases in magnitude and dominates the reaction toward the end of phase

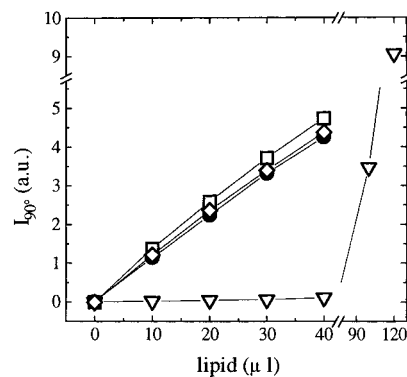


Figure 3. Titration of OG solutions with small unilamellar vesicles of POPC as detected by right-angle light scattering. Detergent solutions ($V = 1.5$ mL; buffer: 10 mM Tris, pH 7.4, 100 mM NaCl; $T = 28$ °C) were titrated with vesicles ($10 \mu\text{L injections}$, lipid concentration $c_L \approx 36$ mM in buffer). The solution was constantly stirred. Both excitation and emission wavelengths were set to 350 nm: (●) buffer, (◇) 5 mM OG, (□) 15 mM OG, (▽) 25 mM OG.

II. The third phase starts after about $2N$ injections and is characterized by a smooth decrease in the reaction enthalpy. However, the heat of reaction, δh_i , is now distinctly smaller than that observed in the first phase of the titration. The cumulative heat of reaction, $\delta H_i = \sum_i \delta h_i$, defined as the sum of the first i titration peaks, is displayed in Figure 2B. The concentration of the phospholipid vesicles used in the titration experiment of Figure 2 was 14.3 mM and was thus about a factor of two smaller than the lipid concentrations used in Figure 1. The heat of detergent dilution was determined in separate dilution experiments. At the highest OG concentration measured (22 mM), the heat of dilution was up to 8% of the measured heat of binding.

Light-Scattering and Phosphorus-31 NMR. The structural changes of the lipid bilayers were monitored with light scattering (Figure 3) and ³¹P-NMR spectroscopy (Figure 4). In a typical light-scattering experiment $10 \mu\text{L}$ aliquots of a lipid suspension ($c_L \sim 35$ mM) were added to OG solutions of different concentrations, and the scattering signal at 90° with respect to the incoming beam was recorded after an equilibration period of 2 min. To a first approximation, the scattering intensity of a sonified vesicle suspension should be linearly dependent on the lipid concentration. Hence, a plot of the scattering intensity vs the lipid concentration should yield a straight line. This is indeed borne out experimentally for the injection of vesicles into buffer without detergent (Figure 3). It can also be expected that an increase in vesicle size due to incorporation of detergent will increase the scattering intensity.

Inspection of Figure 3 demonstrates that this effect is observed experimentally as long as the detergent concentration remains below a critical concentration of 15–16 mM, in agreement with similar findings for the egg yolk lecithin–OG system.¹³ However, a completely different result is obtained for OG solutions at concentrations above this concentration. As is demonstrated in Figure 3, the addition of POPC to an OG solution with $c_{\beta}^0 = 25$ mM produces almost no change in the light scattering during the first few injections. Obviously, the phospholipid vesicles are disrupted, and small OG/POPC micelles are formed which do not produce scattering intensity. Micellization of phospholipid bilayers continues as long as the free OG concentration remains above a critical limit of about 15–16 mM. If the free OG concentration drops below this value, further addition of phospholipid vesicles produces an abrupt increase in the light-scattering intensity (cf. Figure 3) since the concentration of free detergent is too low to achieve solubilization.^{7,13}

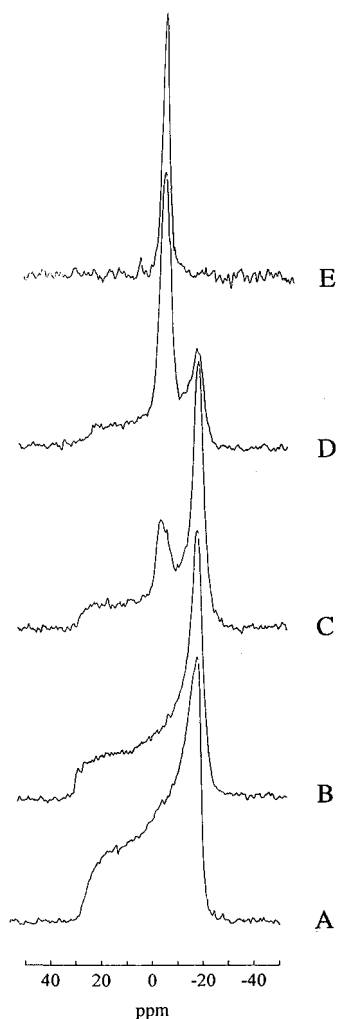


Figure 4. Phosphorus solid state NMR spectra of pure POPC membranes and of POPC in mixture with OG. Samples contained ~ 10 mg of lipid and $50 \mu\text{L}$ of water. The (total) detergent-to-lipid ratio is denoted X_b . (A) POPC (pure lipid), (B) $X_b = 1.3$, (C) $X_b = 1.5$, (D) $X_b = 2.0$, (E) $X_b = 3.4$.

Figure 4 displays ^{31}P -NMR spectra of POPC membranes without detergent (A) and with increasing amounts of detergent (B–E). POPC (~ 10 mg) and defined amounts of detergent were mixed in organic solvent, and the mixture was dried under high vacuum. A small amount of buffer ($\sim 50 \mu\text{L}$) was added which was sufficient to ensure full hydration of the phospholipid membrane. Under these conditions more than 95% detergent can be expected to be incorporated into the membrane phase. The degree of binding, X_b , is thus close to the total detergent/total lipid molar ratio, i.e. $X_b \approx c_{\text{D,b}}^{\circ}/c_{\text{L}}^{\circ}$. Spectrum A, obtained in the absence of detergent, exhibits the shape and the chemical shift anisotropy characteristic of a lipid bilayer.^{20,21} The same holds true for spectrum B obtained for a membrane with an OG-to-POPC molar ratio of $X_b = 1.3$. Apparently, OG can be incorporated into the lipid bilayer up to a very high detergent level without changing the bilayer characteristics.¹⁶ However, increasing the OG concentration beyond $X_b = 1.3$ produces an additional sharp resonance (spectrum C, $X_b = 1.5$; spectrum D, $X_b = 2.0$) which is superimposed on the bilayer spectrum. This so-called isotropic resonance can be explained by a rapid and random movement of phospholipid molecules through all angles of space, indicating the formation of isotropic structures (micelles, cubic phase, small discoidal bilayer fragments). The latter are in slow equilibrium with the bilayer phase. Finally, at detergent-to-lipid ratios of $X_b \geq 2.8$, only the isotropic peak

is observed (spectrum E, $X_b = 3.4$). Under these conditions all bilayer fragments are completely converted into isotropic structures.

Discussion

Solubilization of lipid vesicles by detergent is a rather complex process which involves the uptake of detergent into the lipid bilayer, the formation of intermediary bilayer/micellar structures, and finally the complete micellization of the bilayer. A thermodynamic analysis of this process, based on titration calorimetry, has recently been given for the POPC/octaethylenglycol mono-*n*-dodecyl ether (C_{12}E_8) system.²² The approximate phase boundaries between pure lipid membranes, pure micelles, and mixed micellar/bilayer structures could be deduced.

The POPC/ C_{12}E_8 system differs from the POPC/OG system in two respects. First, the critical micellar concentration of C_{12}E_8 is only 0.07–0.1 mM compared to 20–25 mM for the POPC/OG system. Secondly, the partition constant of C_{12}E_8 is at least one order of magnitude larger than that of OG.^{1,22} Both effects together minimize the concentration of free C_{12}E_8 monomers which can hence be neglected in the analysis of the POPC/ C_{12}E_8 system. In contrast, the concentration of OG monomers in the present work is comparable to those of the other species (mixed micelles, mixed bilayers) which are in equilibrium with OG monomers. The latter must therefore be included in the thermodynamic model.

Thermodynamic Partition Model. At concentrations well below the critical micellar concentration, the association of OG with the lipid membrane can be described by a simple partition equilibrium according to¹⁶

$$X_b = Kc_{\text{D,f}} \quad (2)$$

X_b is the degree of binding and is defined as the ratio of membrane-bound detergent, $c_{\text{D,b}}$, to total lipid, c_{L}°

$$X_b = c_{\text{D,b}}/c_{\text{L}}^{\circ} \quad (3)$$

X_b is also called “surfactant-to-lipid ratio R_e ”.^{7,14} K is the partition coefficient and $c_{\text{D,f}}$ is the free (equilibrium) concentration of surfactant in bulk solution. Taking into account the conservation of mass of the surfactant

$$c_{\text{D}}^{\circ} = c_{\text{D,f}} + c_{\text{D,b}} \quad (4)$$

eq 2 may be rewritten as

$$c_{\text{D,b}} = c_{\text{D}}^{\circ} \frac{Kc_{\text{L}}^{\circ}}{1 + Kc_{\text{L}}^{\circ}} \quad (5)$$

The molar heat of OG partitioning into POPC membranes is $\Delta H_{\text{D}}^{\circ}$, and the measured heat of reaction is given by

$$\delta H = n_{\text{D,b}}\Delta H_{\text{D}}^{\circ} = c_{\text{D,b}}V\Delta H_{\text{D}}^{\circ} \quad (6)$$

V is the total volume of the reaction solution, and $n_{\text{D,b}} = c_{\text{D,b}}V$ is the molar amount of detergent bound to the lipid membrane. In the titration experiment, the lipid concentration in the calorimeter cell is not constant but increases with each injection by

$$\delta c_{\text{L,i}} = V_{\text{inj}}c_{\text{L}}^{\circ}/V \quad (7)$$

After i injections the cumulative heat is given by¹⁶

$$\delta H_i = c_D^{\circ} \Delta H_D^{\circ} V \frac{i K V_{\text{inj}} c_L^{\circ}}{1 + i K V_{\text{inj}} c_L^{\circ}} \quad (8)$$

The reaction volume V also increases with each injection by V_{inj} . The resulting dilution effects can be taken into account with the following substitutions:

$$\begin{aligned} V &\rightarrow V_0 + i V_{\text{inj}} \\ c_L^{\circ} &\rightarrow c_L^{\circ} V_0 / (V_0 + i V_{\text{inj}}) \\ c_D^{\circ} &\rightarrow c_D^{\circ} V_0 / (V_0 + i V_{\text{inj}}) \end{aligned} \quad (9)$$

leading to

$$\delta H_i = c_D^{\circ} \Delta H_D^{\circ} V_0 V_{\text{inj}} \frac{i K c_L^{\circ}}{V_0 + i V_{\text{inj}} (1 + K c_L^{\circ})} \quad (10)$$

The heat change between two consecutive injections δH_{i-1} and δH_i is

$$\delta h_i = \delta H_i - \delta H_{i-1} \quad (11)$$

and is directly accessible in the calorimetric titration. Equations 10 and 11 have been applied successfully to describe the lipid-into-detergent titration curves of octyl- β -d-glucopyranoside¹⁶ and octyl- β -thioglucopyranoside²³ at concentrations *below* the critical micellar concentration. The two free parameters of the model are the partition constant, K , and the partition enthalpy, ΔH_B° . For OG partitioning into POPC membranes they were found to be $K = 120 \pm 10 \text{ M}^{-1}$ and $\Delta H_B^{\circ} = 1.3 \pm 0.15 \text{ kcal/mol}$, providing an excellent fit to a large number of titration curves. The calorimetric titrations were, however, limited to OG concentrations of $c_B^{\circ} \leq 10 \text{ mM}$, and the highest X_b value was $X_b = 1.1$. According to the NMR data (Figure 4), $X_b = 1.3$ is the limit for stable OG/POPC bilayers.

Partition constants have been found to vary with the composition of mixed phospholipid/detergent bilayers.¹ They appear to be large at low surfactant concentrations in the membrane but decrease as detergent-lipid interactions are replaced by detergent-detergent interactions. Since the present studies were performed close to the critical micellar concentration of OG, it can be expected that K and ΔH_B° differ from their respective values deduced for dilute surfactant solutions. In addition, the discontinuities observed in the titration curves cannot be explained by the simple partition model. Nevertheless, we have extended the above partition model to the higher OG concentrations employed in the present work. Figure 5 shows a comparison of experimental results with theoretical simulations. The solid lines were calculated with eqs 10 and 11. K and ΔH_B° were adjusted to provide an optimum fit for the smooth part of the titration curve defining the end of the titration experiment. All titrations could be simulated with very similar parameters, namely $K = 88 \pm 3 \text{ M}^{-1}$ and $\Delta H_B^{\circ} = 1.7 \pm 0.4 \text{ kcal/mol}$ (average of eight titrations). The partition constant is smaller and the partition enthalpy slightly larger than the corresponding parameters of dilute OG solutions.

At the lowest OG concentration measured (15 mM, Figure 5A), the above parameter set provides an almost perfect simulation of the whole titration curve. The degree of binding assumes its maximum value $X_b = 1.312$ at the first lipid injection and decreases with subsequent injections. As revealed by ³¹P-NMR, a surfactant-to-lipid ratio of 1.3–1.4 is the upper boundary for a stable bilayer. Figure 5B displays the analogous simulation for $c_B^{\circ} = 16 \text{ mM}$. The first two injections deviate from the theoretical line and the X_b values predicted from the

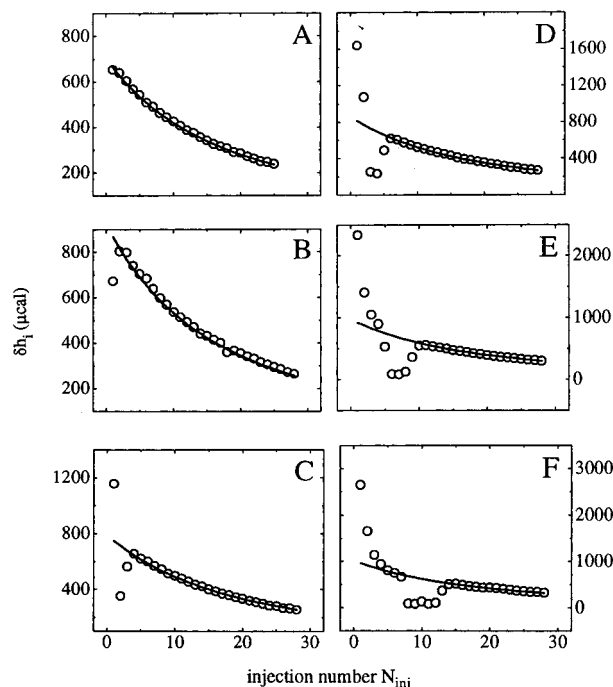


Figure 5. Comparison between experimental titration curves and theoretical predictions based on the partition model $X_b = K c_{D,f}$. The open circles are the experimental titration peaks $\delta h_i = h_i - h_{d,i}$ as measured in Figure 1 (h_i) and corrected for dilution effects ($h_{d,i}$). The solid lines are calculated with the partition model (eqs 10 and 11): (A) OG concentration $c_B^{\circ} = 15 \text{ mM}$, simulation parameter $K = 90 \text{ M}^{-1}$, $\Delta H_B^{\circ} = 1.7 \text{ kcal/mol}$; (B) $c_B^{\circ} = 16 \text{ mM}$, $K = 90 \text{ M}^{-1}$, $\Delta H_B^{\circ} = 1.75 \text{ kcal/mol}$; (C) $c_B^{\circ} = 17 \text{ mM}$, $K = 84 \text{ M}^{-1}$, $\Delta H_B^{\circ} = 1.77 \text{ kcal/mol}$; (D) $c_B^{\circ} = 18 \text{ mM}$, $K = 90 \text{ M}^{-1}$, $\Delta H_B^{\circ} = 1.695 \text{ kcal/mol}$; (E) $c_B^{\circ} = 20 \text{ mM}$, $K = 88 \text{ M}^{-1}$, $\Delta H_B^{\circ} = 1.71 \text{ kcal/mol}$; (F) $c_B^{\circ} = 22 \text{ mM}$, $K = 85 \text{ M}^{-1}$, $\Delta H_B^{\circ} = 1.67 \text{ kcal/mol}$.

partition equilibrium are above the critical limit for these injections. At the third injection, X_b drops to 1.31, and the experimental data agree with the simulation for all following injections.

Bilayer–Micelle Transformation. The discrepancy between theory and experiment becomes quite pronounced at high surfactant concentrations. Inspection of Figure 5 demonstrates that the theoretical curve of the partition equilibrium is the dividing line between two opposite but approximately symmetric effects. The basic process is the OG partitioning into the membrane (solid line). During the first N injections, the endothermic heat due to detergent partitioning is *enhanced* by a second endothermic reaction. In contrast, during the second N injections, the heat of partitioning is *reduced* by an exothermic reaction. After about $2N$ injections the experimental data follow the theoretical prediction for a simple partition equilibrium. This phenomenon is illustrated with higher resolution in Figure 6 for the titration of a 19 mM OG solution with a 14.25 mM POPC suspension (data of Figure 2). The lipid concentration is reduced by a factor of 2 compared to the titrations of Figure 5.

The first 11 injections are characterized by additional endothermic contributions and the total excess heat is +1252 μcal . Since the total amount of injected lipid is 6.65 nmol, this leads to a molar excess enthalpy of $\Delta H_{\text{mic}} = +1.88 \text{ kcal/mol}$ lipid. The exothermic heat of reaction during the consecutive 11 injections is $-1487 \mu\text{cal}$ and thus compensates the endothermic contribution. Indeed, for all other concentrations measured the excess heats above and below the dividing line of the partition equilibrium were found to be identical within 5%. If normalized to the amount of added lipid during the first

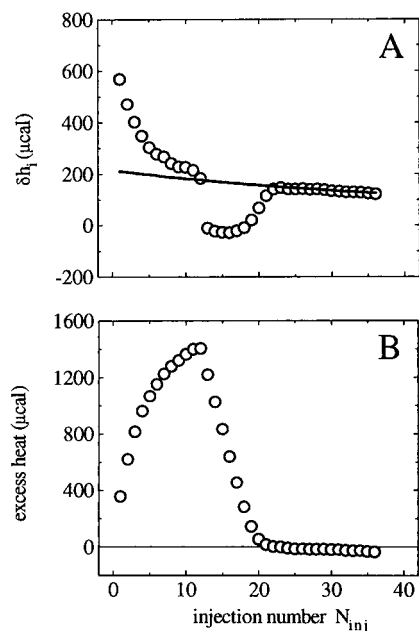


Figure 6. Excess heat of micellization and demicellization. Comparison between experimental heats of titration δh_i and δH_i (open symbol) and theoretical predictions. The experimental data are those of Figure 2, describing the titration of POPC vesicles ($c_L^0 = 14.25$ mM) into an OG solution ($c_B^0 = 19$ mM). The solid line is the theoretical prediction calculated with eqs 10 and 11 using $K = 90$ M $^{-1}$ and $\Delta H_B^0 = 1.75$ kcal/mol. (A) Heats of titration δh_i are shown as a function of the injection number N_{inj} . (B) The variation of the excess heat is shown as a function of N_{inj} . The figure represents the difference between the experimental cumulative heat of reaction, $\delta H_i = \sum \delta h_i$, and the cumulative heat predicted by the partition model, i.e. the difference between the open circles and the solid line in Figure 2B.

N injections, the average values of five different measurements were $\Delta H_{\text{mic}} = +1.85 \pm 0.1$ kcal/mol for the endothermic phase and $\Delta H_{\text{dem}} = -1.84 \pm 0.1$ kcal/mol for the exothermic phase. All experimental titration curves merge with the theoretical partition equilibrium at $X_b = 1.36 (\pm 0.04)$, corresponding to a critical OG concentration of $c_B^0 = 15.4 (\pm 0.3)$ mM.

The three stages of the calorimetric titration can be assigned to three distinct molecular processes. The basic mechanism is a partitioning of surfactant into phospholipid vesicles as described by eq 2. Partitioning occurs during the whole titration experiment and produces an endothermic heat of reaction. However, additional enthalpy contributions come into play due to vesicle micellization and demicellization. If $c_B^0 > c_B^*$, OG partitioning is followed by membrane disruption and the formation of mixed OG/POPC micelles in equilibrium with OG monomers. This process is endothermic and the enthalpy of micellization is $\Delta H_{\text{mic}} = 1.85 \pm 0.1$ kcal/mol lipid. As a comparison it should be noted that (i) the enthalpy of micelle formation of pure OG is $+1.5$ kcal/mol (at 28 °C)^{18,19} and (ii) the temperature-induced bilayer \rightleftharpoons hexagonal phase transition of phospholipids is about 1.5 kcal/mol.²⁴ After N injections the process of micelle formation comes to a halt. Addition of further lipid will shift the bilayer \rightleftharpoons mixed micelle equilibrium toward the bilayer structure and will return the enthalpy consumed in the bilayer \rightarrow micelle transition. The enthalpy of demicellization is $\Delta H_{\text{dem}} = -1.84 \pm 0.1$ kcal/mol lipid. The second phase of the titration experiment is thus characterized by a superposition of an endothermic partition enthalpy and an exothermic heat of demicellization. Inspection of Figure 2 demonstrates that OG partitioning is faster than bilayer formation since the endothermic partition peak precedes the exothermic peak of demicellization.

Micelle formation and demicellization are almost symmetrical processes. This is evidenced by the fact that a similar number of lipid injections is needed for the bilayer \rightarrow micelle and the micelle \rightarrow bilayer transition (cf. Figures 1 and 2). If the free surfactant concentration is below $c_B^* = 15.4$ mM, the reaction mixture no longer contains micelles but only mixed POPC/OG bilayers in equilibrium with OG monomers. The third phase of the titration experiment then corresponds to a pure partition equilibrium. Addition of lipid vesicles produces an endothermic reaction enthalpy due to OG partitioning into the bilayer.

Figures 2B and 6B show the variation of the excess heat of micellization and demicellization as a function of the injection number. A consistent quantitative interpretation of all titration curves can be given by describing the bilayer \rightleftharpoons micelle transition in terms of a simplified mixing model for the surfactant molecules. We distinguish between detergent molecules associated with bilayers (concentration $c_{D,b}^{(i)}$) and detergent molecules available to form mixed lipid/detergent micelles (concentration $c_{D,mic}^{(i)}$). The concentration of the latter is given by

$$c_{D,mic}^{(i)} = c_D^0 - c_D^* - c_{D,b}^{(i)} \quad (12)$$

since no micelles can be formed at concentrations below the critical limit c_B^* . $c_{D,mic}^{(i)}$ and $c_{D,b}^{(i)}$ change with each lipid bilayer injection i . c_B^0 also changes slightly due to dilution effects. $c_{D,b}^{(i)}$ can be calculated from eq 2 and $c_{D,mic}^{(i)}$ is thus also known. The mole fraction of detergent molecules in the micellar phase is

$$X_{D,mic}^{(i)} = \frac{c_D^0 - c_D^* - c_{D,b}^{(i)}}{c_D^0 - c_D^*} \quad (13)$$

and that of detergent molecules associated with the lipid bilayer is

$$X_{D,b}^{(i)} = \frac{c_{D,b}^{(i)}}{c_D^0 - c_D^*} \quad (14)$$

with $X_{D,b}^{(i)} = 1 - X_{D,mic}^{(i)}$. Surfactant molecules in the micellar phase are characterized by a partial molar enthalpy $\tilde{H}_{D,mic}$ and those associated with the lipid bilayer by $\tilde{H}_{D,b}$. Again both parameters will vary with the composition of the system. The excess enthalpy is then given by

$$\delta H = n_{D,mic} \tilde{H}_{D,mic} + n_{D,b} \tilde{H}_{D,b} \quad (15)$$

where $n_{D,mic}$ and $n_{D,b}$ denote the molar amount of surfactant in the respective phase. The *average excess enthalpy*, $\Delta \bar{H}_D^E$, can be defined as²⁵

$$\Delta \bar{H}_D^E = \frac{\delta H}{n_{D,mic} + n_{D,b}} = X_{D,mic} \tilde{H}_{D,mic} + X_{D,b} \tilde{H}_{D,b} \quad (16)$$

$$\Delta \bar{H}_D^E = X_{D,mic} (\tilde{H}_{D,mic} - \tilde{H}_{D,b}) + \tilde{H}_{D,b} \quad (17)$$

Both $\Delta \bar{H}_D^E$ and $X_{D,mic}$ can be measured. Figure 7 then shows a plot of $\Delta \bar{H}_D^E$ vs $X_{D,mic}$ for all measurements performed. Within the accuracy of the measurements, all titration curves lead to the same $\Delta \bar{H}_D^E$ vs $X_{D,mic}$ function.

In so-called simple mixtures the excess function is symmetrical with respect to both mole fractions,²⁶

$$\Delta \bar{H}_D^E = \rho X_{D,mic} X_{D,b} = \rho X_{D,mic} (1 - X_{D,mic}) \quad (18)$$

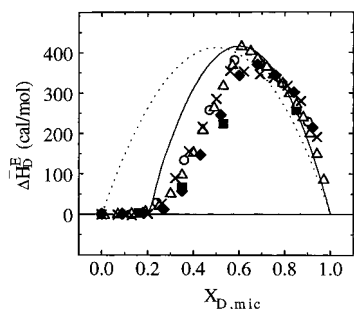


Figure 7. Average excess heat, $\Delta\bar{H}_D^E$, of the bilayer \rightleftharpoons micellization reaction as a function of the mole fraction of micellar detergent, $X_{D,mic}$: (■) total detergent concentration $c_D^0 = 18$ mM (Figure 1C); (○) $c_D^0 = 19$ mM (Figure 1D), (△) $c_D^0 = 19$ mM (Figure 2A); (◆) $c_D^0 = 20$ mM (Figure 1E); (×) $c_D^0 = 22$ mM (Figure 1F).

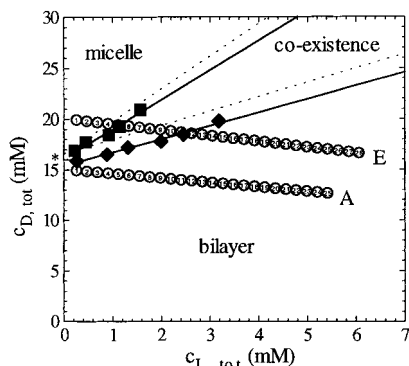


Figure 8. Phase diagram of aqueous mixtures of OG and POPC at 28 °C. The open symbols denote the phase boundaries. They were derived from titrations as shown in Figure 1 as explained in the text. The solid lines are the linear least squares fits to the data. The dotted lines were taken from Almog et al. for a related system of egg lecithin in mixture with OG.⁷ The asterisk marks the critical micellar concentration, $c_{cmc}^0 \sim 16$ mM, of OG in mixtures of POPC. The compositions obtained by the titration experiments presented in Figure 1 (trace A and E) are shown by circles; the enclosed figures indicate the injection numbers.

This function is shown in Figure 7 with $\rho = 1600$ cal/mol (dashed line). A better fit is obtained by

$$\Delta\bar{H}_D^E = \rho\{X_{D,mic}(1.2 - X_{D,mic}) - 0.2\} \quad (19)$$

with $\rho = 2600$ cal/mol. This function has its maximum at $X_{D,mic} = 0.6$. Statistical theories predict that a mixture of two kinds of related nonpolar molecules should show a behavior which is represented by formulas 18 or 19. The bilayer \rightleftharpoons micelle transition approximately fulfills this condition.

Phase Diagram of POPC/OG Mixtures. The thermodynamic analysis suggests a simple scheme to construct an approximate phase diagram for the POPC/OG system at low lipid/detergent concentrations. To this purpose, Figure 8 shows a plot of the total detergent concentration, c_D^0 , vs the total lipid concentration, c_L^0 , for two experiments taken from Figure 1. While the total amount of detergent in the calorimeter cell remains constant, the concentration, c_D^0 , decreases slightly due to the dilution effect of the added lipid suspension. The open circles represent the experimental data points, numbered in the order of injection. The solid symbols indicate the discontinuities in the titration experiment. Experiment A shows no discontinuities. In contrast, experiment E exhibits two phase changes. The first one, at low c_L^0 , defines the boundary between purely micellar structures and the micelle/bilayer coexistence region; the second one, at high c_L^0 , defines the phase boundary between the coexistence region and the pure bilayer phase. From the remaining experiments of Figures 1 and 2 only those data points

were included which characterize the discontinuities in the titration curves. The two solid lines then define the phase boundaries. Linear regression analysis leads to

$$c_D^0 \approx 16.2 + 2.8c_L^0 \text{ (mM)} \quad (20)$$

for the boundary between the micellar phase and the bilayer/micelle coexistence phase. The boundary between the bilayer/micelle coexistence phase and the pure bilayer phase is given by

$$c_D^0 \approx 15.4 + 1.31c_L^0 \text{ (mM)} \quad (21)$$

The light-scattering data are in agreement with the phosphorus-31 NMR data which show the formation of a pure isotropic phase at an OG/POPC ratio > 2.8 and a bilayer \rightleftharpoons mixed bilayer–micelle transition at an OG/POPC ratio > 1.31 .

Also included in Figure 8 are the phase boundaries for the egg-yolk lecithin-octyl- β -D-glucopyranoside system, derived from turbidity measurements.^{7,27} The major component of egg-yolk lecithin is POPC ($\sim 65\%$) and the figure demonstrates the close similarity of the two phase diagrams. Equation 21 which describes the phase boundary between the bilayer phase and the bilayer–micelle coexistence phase lends itself to a simple theoretical interpretation. Using eqs 4 and 5 the free (equilibrium) detergent concentration is given by

$$c_{D,f} = c_D^0 / (1 + Kc_L^0) \quad (22a)$$

or

$$c_D^0 = c_{D,f}(1 + Kc_L^0) \quad (22b)$$

At the phase boundary between the pure bilayer phase and the bilayer–micelle coexistence phase, $c_{D,f}$ reaches the critical limit c_D^* leading to

$$c_D^0 = c_D^* + Kc_D^*c_L^0 \quad (23)$$

which can be identified with eq 21. From $c_D^* = 15.4$ mM and $Kc_D^* = 1.31$ we obtain $K = 85 \text{ M}^{-1}$, in excellent agreement with the simulation of the titration curves described above. It should be noted that eq 23 allows a determination of the partition constant, K , without knowledge of the partition enthalpy.

Application of eq 23 is not limited to titration calorimetry. Using turbidity measurements, Almog et al. have studied the phase diagram of octyl- β -D-glucopyranoside in mixture with egg-yolk phosphatidylcholine.⁷ The detergent level at which solubilization began was determined as $D_T^{\text{sat}} = 16.6 + 1.4[\text{PC}]$ (detergent and lipid concentration given in mM) which can be identified with eq 23. The OG partition constant is derived as $K = 84 \text{ M}^{-1}$, in agreement with earlier centrifugation assays^{11–13} and recent calorimetric data¹⁶ on the same system.

Conclusions

The thermodynamic analysis was facilitated by the high micellar concentrations and the low detergent–lipid partition constant of the POPC/OG system. Under these conditions it was possible to visualize membrane partitioning, membrane micellization, and membrane formation as three different stages in the titration curves. A quantitative description of the titration pattern was achieved by combining OG partitioning with bilayer micellization or bilayer formation. The minimum OG concentration to induce POPC micelle formation was $c_D^0 = 15.4 \pm 0.3$ mM and was smaller than the critical micellar concentration of pure OG solutions with $c_{cmc} \approx 23.7$ mM (in buffer). The phase boundary between the bilayer phase is characterized by $X_b =$

1.36 ± 0.04 and $c_{D,f} = 15.4$ mM. The bilayer \rightleftharpoons micelle transformation enthalpy was endothermic with $\Delta H = 1.85$ kcal/mol lipid and is thus closely related to the bilayer \rightleftharpoons H_{II} phase transition. Measurement of the titration curves at different OG concentrations leads to a precise phase diagram and also to a simple evaluation of the partition constant K .

References and Notes

- (1) Lasch, J. *Biochim. Biophys. Acta* **1995**, *241*, 269.
- (2) Racker, E. *Methods Enzymol.* **1979**, *55*, 699.
- (3) Mimms, L. T.; Zamighi, G.; Nozaki, Y.; Tanford, C.; Reynolds, J. A. *Biochemistry* **1981**, *20*, 833.
- (4) Schurtenberger, P.; Mazer, N.; Waldvogel, S. *Biochim. Biophys. Acta* **1984**, *775*, 111.
- (5) Schubert, R.; Wolburg, H.; Schmidt, K. H.; Roth, H. J. *Chem. Phys. Lipids* **1991**, *58*, 121.
- (6) Lichtenberg, D.; Robson, R. J.; Dennis, E. A. *Biochim. Biophys. Acta* **1983**, *737*, 285.
- (7) Almog, S.; Litman, B. J.; Wimley, W.; Cohen, J.; Wachtel, E. J.; Barenholz, Y.; ben-Shaul, A.; Lichtenberg, D. *Biochemistry* **1990**, *29*, 4582.
- (8) Vinson, P. K.; Talmon, Y.; Walter, A. *Biophys. J.* **1989**, *56*, 669.
- (9) Walter, A.; Vinson, P. K.; Kaplun, A.; Talmon, Y. *Biophys. J.* **1991**, *60*, 1315.
- (10) Stubbs, G. W.; Smith, H. G.; Litman, B. J. *Biochim. Biophys. Acta* **1976**, *426*, 46.
- (11) Jackson, M. L.; Schmidt, C. F.; Lichtenberg, D.; Litman, B. J.; Albert, A. D. *Biochemistry* **1982**, *21*, 4576.
- (12) Lichtenberg, D. *Biochim. Biophys. Acta* **1985**, *821*, 470.
- (13) Ollivon, M.; Eidelmann, O.; Blumenthal, R.; Walter, A. *Biochemistry* **1988**, *27*, 1695.
- (14) De la Maza, A.; Parra, J. L. *Eur. J. Biochem.* **1994**, *226*, 1029.
- (15) Eidelman, O.; Blumenthal, R.; Walter, A. *Biochemistry* **1988**, *27*, 2839.
- (16) Wenk, M. R.; Alt, T.; Seelig, A.; Seelig, J. *Biophys. J.* **1997**, *72*, 1719.
- (17) Wiseman, T.; Willington, S.; Brandts, J. F.; Lung-Nan, L. *Anal. Biochem.* **1989**, *179*, 131.
- (18) Paula, S.; Süß, W.; Tuchtenhagen, J.; Blume, A. *J. Phys. Chem.* **1995**, *99*, 11742.
- (19) Antonelli, M. L.; Bonicelli, M. G.; Ceccaroni, G.; La Mesa, C.; Sesta, B. *Collid Polym. Sci.* **1994**, *272*, 704.
- (20) Niederberger, W.; Seelig, J. *J. Am. Chem. Soc.* **1976**, *98*, 3704.
- (21) Seelig, J. *Biochim. Biophys. Acta* **1978**, *505*, 105.
- (22) Heerklotz, H.; Lantzsch, G.; Binder, H.; Klose, G.; Blume, A. *J. Phys. Chem.* **1996**, *100*, 6764.
- (23) Wenk, M. R.; Seelig, J. *Biophys. J.*, manuscript submitted for publication.
- (24) Seddon, J. M.; Cevc, G.; Marsh, D. *Biochemistry* **1983**, *22*, 1280.
- (25) Kortüm, G. *Einführung in die chemische Thermodynamik*, 6th ed.; Verlag Chemie: Weinheim, Germany, 1972, p 136.
- (26) Guggenheim, E. A. *Thermodynamics*, 5th ed.; North-Holland Publishing Co.: Amsterdam, 1967, p 196.
- (27) da Graca Miguel, M.; Eidelman, O.; Ollivon, M.; Walter, A. *Biochemistry* **1989**, *28*, 8921.